Nematic Elastomer Fiber Actuator

Jawad Naciri,*,† Amritha Srinivasan,† Hong Jeon,† Nikolay Nikolov,† Patrick Keller,‡ and Banahalli R. Ratna†

Center for Bio/Molecular Science and Engineering, Naval Research Lab, 4555 Overlook Avenue SW, Code 6950, Washington, D.C. 20375, and Laboratoire Physico-Chimie Curie, CNRS-UMR 168, Institut Curie-Section de Recherche, 11 rue P. et M. Curie, 75231 Paris Cedex 05, France

Received July 2, 2003; Revised Manuscript Received September 3, 2003

ABSTRACT: We report the synthesis and physical studies of a liquid crystalline elastomer fiber consisting of two side-chain liquid crystalline acrylates and a nonmesogennic comonomer side group that acts as a reactive site for cross-linking. The terpolymer was synthesized by radical polymerization, and the cross-linking of the network was achieved by using a diisocyanate unit. The fiber formed shows good liquid crystal alignment texture under a cross-polarizer microscope. Thermoelastic response shows strain changes through the nematic−isotropic phase transition of about 30−35%. A retractive force of nearly 300 kPa was measured in the isotropic phase. Static work loop studies show the viscoelastic losses in these materials to be very small. We also present preliminary studies on the effect of doping carbon nanotubes on the induced strain at the nematic−isotropic transition.

Introduction

There has been considerable effort to develop human-made actuator materials that can mimic muscle performance.[1,2] The developmental goal is to generate large mechanical actuation induced by external stimuli such as electric field, temperature, and light. Because of their anisotropic orientational symmetry in combination with rubber elasticity, liquid crystal (LC) elastomers are promising materials for applications in the field of sensors and actuators. The potential for liquid crystalline to exhibit unusual properties was first suggested by de Gennes.[3] Subsequently, such elastomers have been prepared and their resultant properties investigated.[4−19] In general, the elastomers most frequently studied have been those based on side-chain liquid crystalline polymers rather than the main-chain systems considered originally by de Gennes. These elastomers exhibit anisotropic shape change under applied fields[5,19,20] as they go through phase transitions and retain network memory[9] which enables them to reversibly contract and extend. There are two basic approaches to prepare LC elastomers: the first approach developed by Mitchell and co-workers[21] involves cross-linking an acrylate polymer prealigned in a magnetic field. Such samples are found to show complete recovery from their global orientation on cooling to the nematic phase from the isotropic phase. The second method due to Finkelmann and co-workers[5,20] involves a two-step cross-linking strategy of a siloxane liquid crystal polymer. The first stage involves a lightly cross-linking of the polymer while applying a stress field. Subsequently, a second cross-linking reaction is performed which fixes the uniaxial alignment. By this method LC elastomers of large dimensions with permanent alignment and highly anisotropic mechanical properties were produced. An alternative approach to the use of chemical reactions to produce intermolecular cross-linking is photo-cross-linking.[22−24] Although such materials show promises for the generation of elastomers, there may be a number of problems associated with their use.[22]

Scheme 1. Concept of Liquid Crystal Elastomer as Artificial Muscle

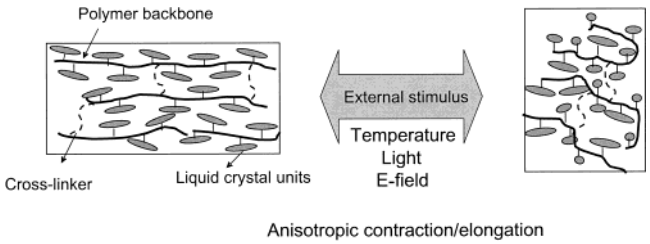

The coupling between the liquid crystalline side group and the polymer backbone is critical for the thermostrictive behavior of elastomeric materials. Theoretical[25,26] and experimental[27,28] studies have shown that orientational order of the side groups will be accompanied by some level of orientational order in the polymer backbone. We have chosen to study elastomers with laterally affixed liquid crystal mesogens (Scheme 1), since they have been shown to exhibit large backbone anisotropy.[28,29]

In our previous paper[19] we presented detailed studies of mechanical properties of two LC elastomer films. These networked films exhibited musclelike physical properties with strains of 35−40% and blocked stress values of the order of 200 kN/m^2.

The subject of this paper is to expand our previous work to the preparation of ordered fibers. The idea of preparing artificial muscles in the form of fibers is based, in part, on its similarity to the way the natural muscles are organized in bundles of fibers. It is well-known that the LC mesogens are spontaneously ordered during the spinning of the fiber.[30,31] Therefore, in the elastomer with side-on attachment of the liquid crystal mesogen, one expects the orientational order of the mesogen as well as the polymer backbone to be along the fiber axis. Hence, we expect the contraction to occur along the fiber axis similar to what occurs in natural muscle fibers. One can envisage using bundles of these fibers in devices, the number of fibers in each bundle

† Naval Research Lab.
‡ Institut Curie-Section de Recherche.
* Corresponding author: e-mail Jnaciri@ccs.nrl.navy.mil, Tel 202-404-6056.

10.1021/ma034921g CCC: $25.00
Published on Web 10/09/2003

dictating the force that needs to be generated. Here, we describe a method for preparing LC fibers from a side chain liquid crystalline terpolymer containing two side-chain mesogens and a nonmesogenic group that acts as a reactive site for cross-linking. The initial cross-linking is allowed to occur in the gel phase, and the sample is mechanically stretched to obtain a monodomain sample before the cross-linking is complete. Thermoelastic and isostrain studies performed as a function of temperature across the nematic−isotropic phase transition of the fiber drawn from a mixture of the terpolymer with the cross-linker will be presented to show that the fiber can mimic some of the mechanical properties of the natural muscle.

Experimental Section

Materials and Techniques. 4-Hydroxybutyl acrylate inhibited with hydroquinone, 4,4′-methylenebis(phenyl isocyanate) (MDI), and anhydrous toluene were obtained from Aldrich. Single-wall carbon nanotubes were purchased from Carbon Nanotechnologies, Inc. (Houston, TX). Prior to polymerization, hydroquinone was removed from 4-hydroxybutyl acrylate using an inhibitor removal column (Column DHR-4 from Scientific Polymer Products, Inc.). Analytical TLC was conducted on Whatman precoated silica gel 60-F254 plates. Molecular weight was determined by GPC using a Shimadzu LC-10A liquid chromatograph equipped with Plgel 5 μm Mixed-D column. THF was used as as the mobile phase and polystyrene as standard. GC/FID sample analysis was carried out on a HP 6890 instrument equipped with a 30 m DB-5 column, with an oven program of 50 °C (1 min) to 300 °C (10 min) at a rate of 8 °C/min. ^{1}H NMR spectra were recorded on a Bruker DRX-400 spectrometer. All spectra were run in $CDCl_3$ solution.

Thermal Analysis. A Perkin-Elmer differential scanning calorimeter DSC 7 equipped with a CCA 7 liquid nitrogen-cooling accessory was used to study the nematic−isotropic phase transition of the monomers and their corresponding polymers. Scans were done at 2 °C/min heating and cooling rate over a temperature range of 0−110 °C. The melting temperature of indium was used as a standard for temperature calibration, which agreed to within 1 deg of the expected value.

Mechanical Studies. All measurements were done on a TA Instrument DMA 2980 with tension clamp for thermoelastic and stress/strain measurements. The clamp assembly consists of a fixed upper clamp and a mobile lower clamp activated by an air bearing under pressure. The fiber was positioned between the two clamps and held under a preload of 0.001 N. The force was increased at the rate of 0.001 N/min, and the corresponding stress−strain values were measured. Thermoelastic experiments follow the length change as a function of temperature. The % strain vs temperature data were collected while the temperature was ramped up (heating cycle) and down (cooling cycle). Isostrain experiments involve heating the fiber while holding it under a predetermined strain. The stress values are measured while the fiber is taken through the nematic−isotropic transition at a constant of 0.5 °C/min.

Synthesis. The syntheses of the monomers MAOC4 and MACC5 were described elsewhere.[19] But here we discuss the synthetic steps used to prepare the terpolymer and the subsequent cross-linking using MDI material.

Polymerization of (4″-Acryloxybutyl) 2,5-Di(4′-butyloxybenzoyloxy)benzoate (MAOC4) and *(4″-Acryloxyloxybutyl) 2,5-Di(4′-pentylcyclohexylcarboxyloxy)benzoate (MACC5)* with *4-Hydroxybutyl Acrylate.* A mixture of MAOC4 (0.25 g, 0.4 mmol), MACC5 (0.38 g, 0.6 mmol), 4-hydroxybutyl acrylate (0.014 g, 0.10 mmol, 10%), and 1.56×10^{-3} g (0.0094 mmol, 1%) of azobis(isobutyronitrile) (AIBN) were dissolved in 8 mL of toluene. The mixture was purged with nitrogen for 30 min to remove oxygen from the solution. The flask was immersed in an oil bath preset at temperature of 65 °C. After heating overnight, the solution was poured in methanol. The polymer was purified by successive reprecipitation from THF solutions into methanol until TLC analysis shows no traces of unreacted monomers. The polymer was dried in a vacuum oven for 24 h to yield 0.5 g of white waxy material. ^{1}H NMR ($CDCl_3$): 0.8−2.6 (m, 77H aliph), 3.42−4.1 (m, 16H, 8CH_2−O), 6.84−8.0 (m, 14H, ArH). The signal from olefinic hydrogens, which indicate the presence of the acrylic group, had completely disappeared from the NMR spectrum. The molecular mass determined from GPC (THF, polystyrene standard) was found to be $M_w = 30\,000$ mol/g and $M_n = 19\,200$ mol/g. The density of the hydroxybutyl group present in the polymer was indirectly determined by using the GC technique. A small amount of the mixture before and after polymerization was taken and injected into a GC instrument. The mixture consists of MAOC4, MACC5, hydroxybutyl acrylate, toluene, and cyclohexanone (reference standard). Comparison of the area under the peaks for cyclohexanone and hydroxybutyl acrylate compounds before and after polymerization shows that all the cross-linker has been consumed.

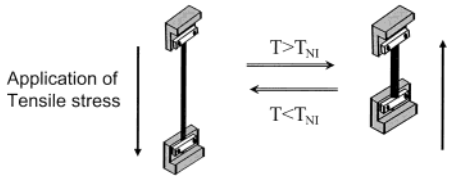

Figure 1. Schematic of the clamping system used in the DMA setup.

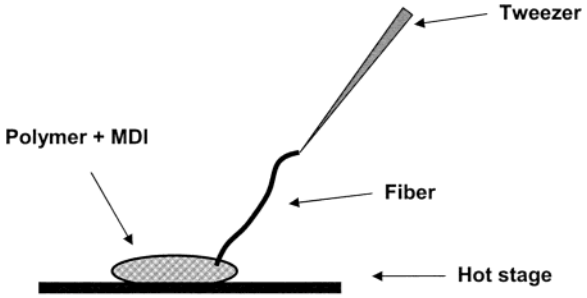

Figure 2. Schematic of the setup used for the preparation of the fiber.

Preparation of Liquid Crystal Elastomer (LCE) Fibers. Fibers were drawn from a melt mixture of the polymer and MDI cross-linker. In a typical experiment, a small amount of the polymer (0.04 g) is heated to 80 °C in a microscope slide placed on a thermal stage (Figure 2). A known amount of MDI (0.25/1 mole ratio of MDI relative to the hydroxyl unit present in the polymer backbone) was added at this temperature. Using a concentration higher than 0.25 mol of MDI led to a brittle and inhomogeneous fiber. The temperature was then dropped to around 60 °C, and the sample was mixed well at this temperature (about a minute) until the mixture appears homogeneous. At this point, the mixture becomes viscous, indicating that the cross-linking has started to occur.The fibers were drawn by dipping the tip of a metallic tweezer and pulling the mixture with it as quickly as possible as shown schematically in Figure 2. The fibers were left at room temperature for about 120 h, time over which the cross-linking reaction is completed. The average diameter of the fiber drawn this way was about 300 μm.

Carbon Nanotubes Doped Fiber. A solution of single-walled nanotubes (5 mg) in dichloromethane, terpolymer (30 mg), and MDI (0.62 mg) was stirred for 2 h at room temperature. The solvent was evaporated under vacuum, and the fiber was drawn from a melt at 60 °C as described above.

Results and Discussion

To be able to use a LC elastomer as an artificial muscle, important issues have to be addressed, namely, the temperature range over which the actuation will

Scheme 2

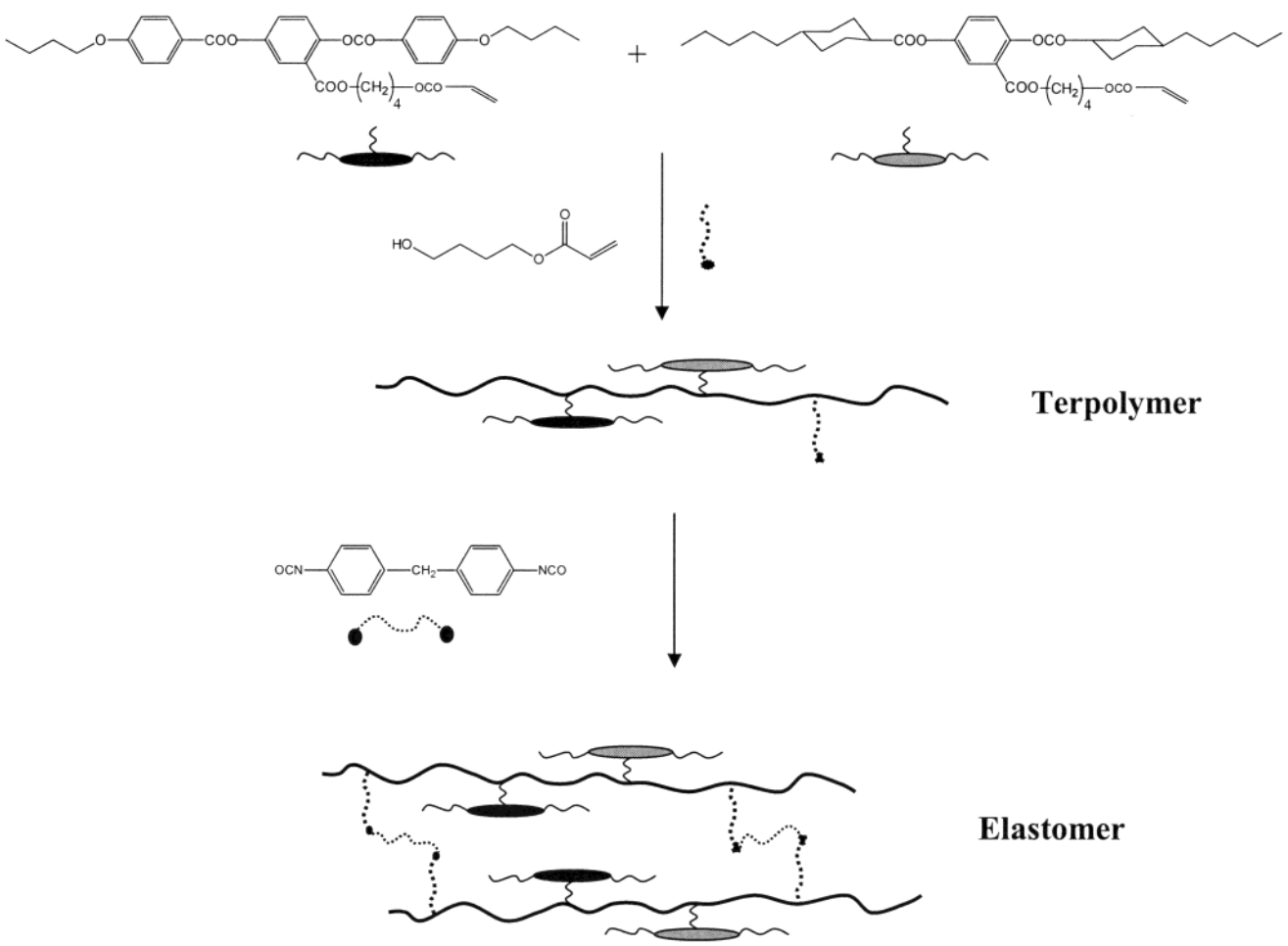

occur, the orientation of the side-chain mesogen within the network so that the strain occurs along the fiber axis, the force generated by the artificial muscle, the performance (energy loss and work generated), and the response time of the actuator. We will address each of these points in the following paragraphs.

Phase Behavior. The synthesis of the nematic liquid crystal terpolymer and the corresponding cross-linked fibers are shown in Scheme 2. The terpolymer was synthesized by free-radical polymerization of two side-chain monomers MAOC4 and MACC5 in a specific molar concentration, namely 40/60 mol % ratio, and a nonmesogenic comonomer with a terminal hydroxyl group that acts as reactive site for cross-linking. The choice of this specific ratio was made on the basis of the studies of the phase diagram of the two monomer mixtures. Figure 3 shows a plot of the nematic-to-isotropic transition temperatures of a series of mixtures of the two mesogens with different compositions, as measured by DSC.

The figure also shows the transition temperatures of the terpolymers prepared from the two monomers and the hydroxyl pendent group. The concentration of the nonmesogenic hydroxyl group was kept constant at 10 mol % for all of terpolymers. In this paper, we have focused our studies on a 40/60 mol % of MACC4/MACC5 in the terpolymer because of its reasonably low N−I and glass transition temperatures combined with the ability of drawing smooth fibers from this sample. The cross-linking component of the network is a reactive difunctional unit, the widely used 4,4′-methylenebis(phenyl isocyanate).[8b] Fibers were drawn at 60 °C in the liquid crystalline phase. The time required for the fiber to be cross-linked completely was found to be approximately 120 h (see below). Phase transition behavior of the monomers, terpolymer, and fibers was characterized by DSC. The phase transition temperatures on cooling are given in Table 1 along with the chemical composition of the polymers.

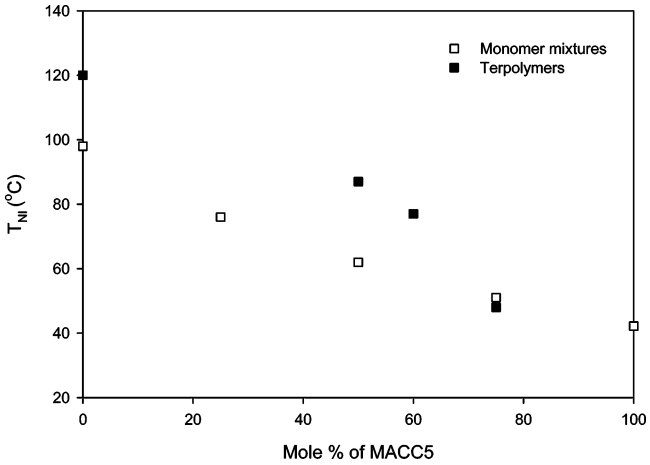

Figure 3. Phase diagram of LC monomer mixtures and terpolymers.

The isotropic-to-nematic transition of MACC5 is monotropic. The terpolymer and the elastomer exhibit an enantiopropic phase transition between the nematic and isotropic phases. The polymerization and cross-

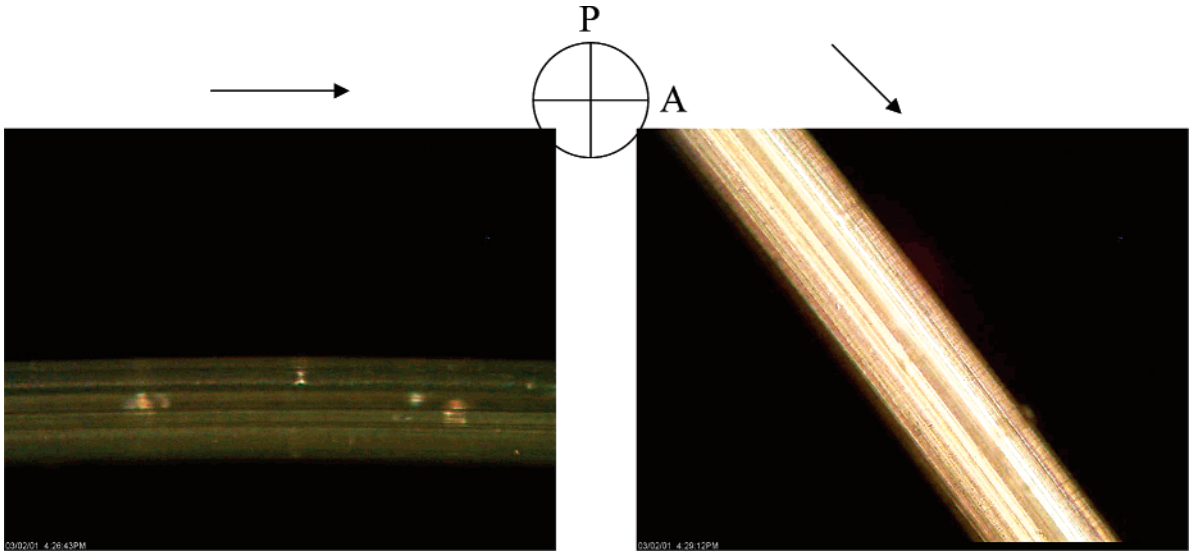

Figure 4. Microphotographs of LC fiber under cross-polarizers.

Table 1. Phase Transition Temperatures of Materials Studied As Determined from DSC

material	T_g (°C)	T_{IN} (°C)	MAOC4 (mol %)	MACC5 (mol %)
MAOC4	71.9 (T_{KN})	98.3		
MACC5	74.0 (T_{KI})	42.2		
terpolymer	28	77	40	60
fiber (10% cross-linker)	33	79.6	40	60

linking processes stabilize the nematic phase. The liquid crystal elastomer fiber displayed textures in the optical microscope which correspond to a nematic phase with a good alignment of the molecular director along the fiber axis (Figure 4). The figure shows a LC fiber placed between cross-polarizers at room temperature. The uniform birefringence observed upon rotating the sample to a 45° position with respect to the analyzer shows that the molecules are well oriented along the fiber axis in the sample. On the basis of the earlier neutron scattering[32,33] on similar LC side-chain polymers, one can expect conformational constraints on the backbone and a concomitant anisotropy in the polymer chain and therefore a contraction along the fiber axis.

Theoretical studies by Warner et al.[26] have suggested how this coupling might affect the phase behavior of LC elastomers. Cross-linking the polymer, which introduces network points that are chemically immobile, can enhance this coupling. As a result, although there is some flexibility in the chain between network points, the introduction of such fixed points imposes additional stability on those conformations present at the time of cross-linking.

Thermoelastic and Isostrain Measurements. We have evaluated the mechanical properties of our fibers. A stress vs strain plot of a fiber left at room temperature for 120 h and measured along the optic axis of the fiber is shown in Figure 5. The measurement was done at 50 °C at force ramp rate of 0.005 N/min, with a 3.2 kPa preload stress. Initially, the slope of the stress−strain curve is approximately linear. The stress reaches a maximum value at which it remains constant before it reaches the breaking point of about 1.5 MPa. The time required for the fiber to be cross-linked completely was found to be approximately 120 h. This result is based on the fact that beyond this time the Young's modulus (E_m) did not change. E_m was determined in the nematic

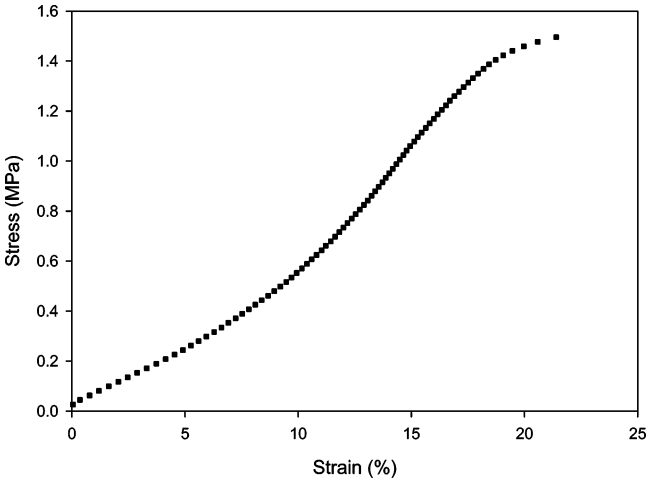

Figure 5. Stress−strain curve for fiber kept at room temperature for 5 days. Measurements were done at 50 °C with a preload stress of 3.2 kPa at a force ramp rate of 0.005 N/min.

phase from the initial slope at small stress values and was found to be 4.37 MPa. The cross-linking density n of the fiber was estimated at low strain values using the equation $E = 3nRT$, where E is Young's modulus measured in the isotropic phase, R is gas constant, and T is temperature. The calculated cross-linking density was found to be 0.9×10^{-4} mol/cm^3.

Thermoelastic studies performed on both heating and cooling cycles at 0.5 °C/min rate are shown in Figure 6 for four values of applied stress. The strain was measured as a function of temperature at constant applied stress over a temperature range covering the nematic-to-isotropic phase transition. The length of the fiber remains constant well in the nematic phase and starts to slowly decrease as the isotropic phase is approached.

At the nematic-to-isotropic phase transition, a sharp decrease in length of ∼30−35% is observed followed by a slow decrease into the isotropic phase (Figure 6). On cooling the process is reversed with a sharp increase in length on going from the isotropic-to-nematic phase. After each heating/cooling cycle, the temperature was equilibrated for 3 min before increasing the stress value, and the next cycle was performed after an isothermal hold for another 3 min. The upward shift of the curves with increasing applied stress is due to the increase in

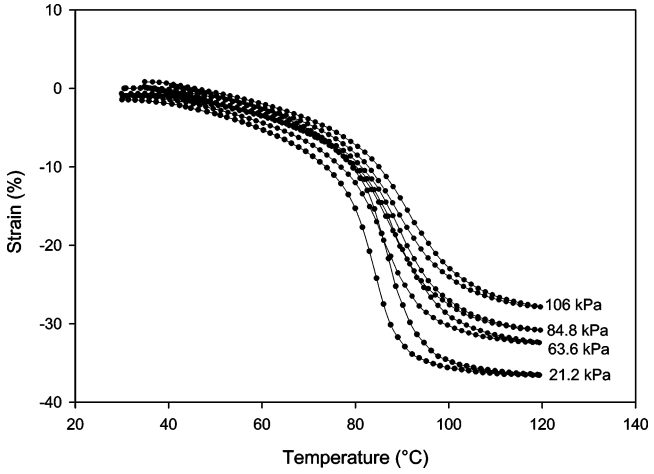

Figure 6. Thermoelastic measurements of aligned fiber at 0.5 °C/min heating and cooling cycles.

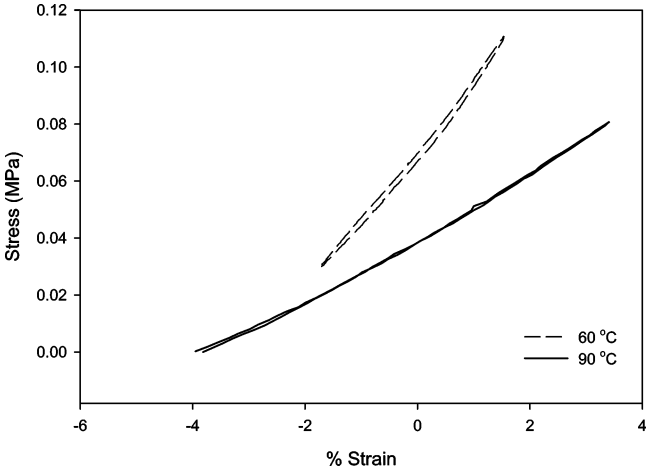

Figure 7. Passive work loops measured at 60 and 90 °C.

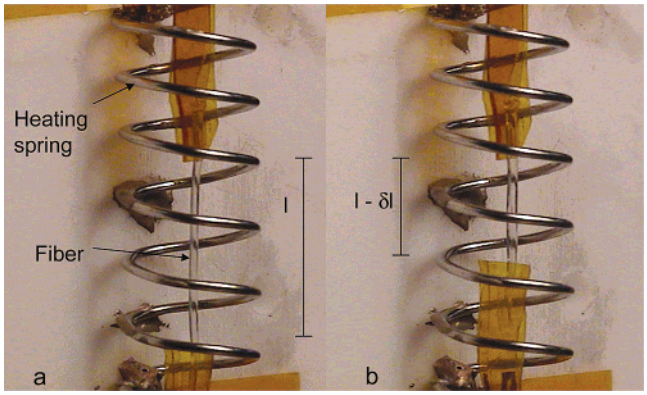

Figure 8. Fiber actuation under a load of 0.002 N. 200 mg weight attached to the bottom end of the fiber is not seen. The fiber is in (a) the extended state in the nematic phase and (b) contracted state in the isotropic phase. The fiber regains its original length on cooling.

length on stretching. An increase is observed in the temperature at which the maximum contraction/extension occurs which is predicted by the phenomenological Landau model for a homogeneous elastomer under an aligning stress.[34] The smooth variation of the induced strain is a result of a similar variation in the order parameter.[35] In an earlier paper,[36] we have tried to explain this smooth variation instead of first-order-like discontinuity at the N−I transition using a modified Landau theory based on the earlier work by de Gennes[3] to be a result of the presence of quenched disorder in the elastomer and the internal stress developed during network formation. Extensive work on molecular theories by Warner and his collaborators[37−41] provides a more accurate description of the large strains near the N−I transitions induced by thermal or photoisomerization processes.

Isostrain measurement was carried out on the fiber by maintaining a constant strain on the material and measuring the force generated as a function of temperature. The retractive force developed in the fiber as it is heated through the nematic-to-isotropic phase transition was measured by holding the fiber at constant length with a known strain imposed on it. As the orientational order is decreased with increasing temperature, the conformational constraint on the polymer network is relaxed, and its effect on an unconstrained elastomer would be to change its shape. However, in this experiment, since the length of the elastomer is held constant, a retractive force develops as the temperature is increased. The maximum retractive force measured in the isotropic phase at a constant strain of 3% was 274 kPa.

If an elastomer has to be used as an actuator to generate work, the material has to overcome viscoelastic losses. Large energy losses can seriously affect the performance of the material or can even make them unusable. The viscoelastic losses can be determined by performing cyclic scans of force vs strain. These scans generate passive work loops which move clockwise, and the area enclosed by the loops is a measure of the viscoelastic losses.[42] Figure 7 shows the work loops performed on the elastomer by varying the force on the fiber at 0.001 N/min in the nematic and isotropic phases. Multiple cycles were performed, showing no increase in the area of the loop. The work loops moved in a clockwise direction, which indicates that the work is absorbed rather than produced over a cycle. The amount of energy absorbed, which represents the viscoelastic losses in the elastomer, is represented by the area within the loop. This was calculated to be 0.085 J/kg at 60 °C. At 90 °C, the loss was even smaller and not measurable. In comparison, VHB 4910 acrylic and CF19-2186 silicone elastomers show a viscoelastic loss[43] of 13.17 and 3.19 J/kg, respectively, values which are much larger than that measured in our material. This indicates that the material exhibits a springlike behavior with negligible losses during the passive work loop. Currently, we are developing methods to evaluate the work generated by the artificial muscle using active work loops and will be published elsewhere.

To demonstrate that the fiber is capable of producing useful work, we have put together a simple device in which the fiber is mounted inside a heating coil, as shown in Figure 8. The upper end of the fiber (12.6 mm long and 0.3 mm in diameter) is fixed, and a 200 mg load is attached to the lower end. The fiber is heated by passing current through the Nichrome coil. When the temperature is increased above the nematic−isotropic transition temperature, the fiber contracts and is able to lift the weight. The induced strain is 40% of the original length.

Carbon Nanotubes Doped Fibers. The actuation in the liquid crystal elastomer described here is induced by a temperature change. The strain rate of these types of thermostrictive materials is mostly dictated by the thermal conductivity of the material.[44] In our earlier

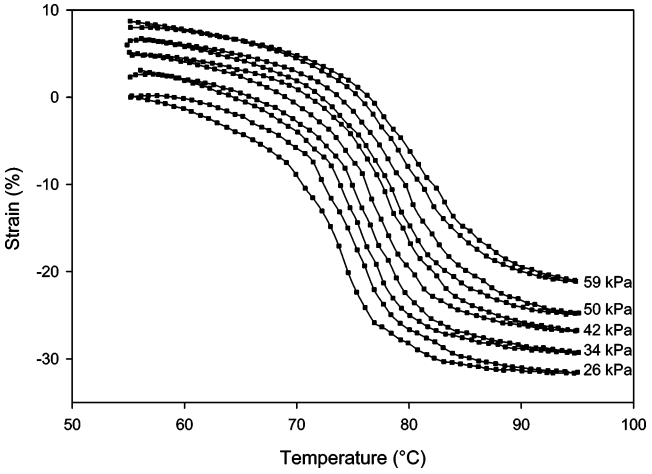

Figure 9. Thermoelastic measurements of LCE fiber doped with nanotubes.

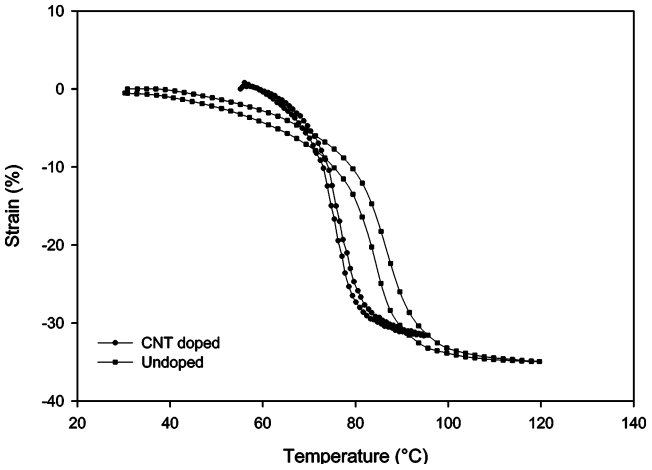

Figure 10. Comparison of strain variation with temperature between CNT doped and undoped fibers at 34 kPa.

effort to improve the thermal conductivity, we have shown that carbon coating of LCE is an effective approach to enhance the response of an elastomer film to an external stimulus. We have demonstrated that the fast conduction of the heat generated in the carbon coating by absorption of infrared laser radiation through the film leads to a significant reduction in the actuation time.[44] In this work, we have been able to dope the fibers with carbon nanotubes without affecting the mechanical properties of the liquid crystal elastomer.

Thermoeslastic studies performed on fiber doped with nanotubes in both heating and cooling cycles at 0.5 °C rate are shown in Figure 9 for five applied stress values. The results are qualitatively similar to that of undoped fiber with a large strain observed at the nematic−isotropic phase transition. Figure 10 is a comparative plot of the two fibers at 34 kPa, showing that the doping does not adversely affect the strain value. In fact, we observe two positive effects of doping: decrease in transition temperature and sharpening of the transition with a smaller hysteresis.

Conclusions

We have shown that nematic elastomers can be drawn into well-oriented fibers which can exhibit musclelike physical properties with an elongation up to 35% and blocked stress of 280 kPa, numbers which are very similar to that exhibited by skeletal muscles. The viscoelastic losses in this elastomer are very small, suggesting that the material acts like a spring. The elastomer can be doped with thermally conducting carbon nanotubes without affecting the mechanical properties. Additional experiments with regard to active work loops, stability, and optimization of the modulus of elastomer have to be carried out in order to consider these materials as artificial muscle actuators.

Acknowledgment. The authors acknowledge financial support from DARPA Controlled Biological and Biomimetric Systems Program. The authors thank Dr. Dev Shenoy for helpful discussions.

References and Notes

(1) Pratt, G. A.; Williamson, M. M.; Dillworth, P.; Pratt, J.; Wright, A. In *Stiffness isn't everything [robots]*; Khatib, O., Salisbury, J. K., Eds.; *Experimental Robotics IV. 4th International Symposium, Proceeding of 4th International Symposium on Experimental Robotics 4, Stanford, CA, 30 June−2 July 1995*; Springer-Verlag: Berlin, Germany, 1997; pp 253−62.
(2) Chou, C.-P.; Hannaford, B. Measurement and modeling of MCkibben Pneumatic Artificial Muscle. *IEEE Trans. Robotics Automation* **1996**, *12*, 90.
(3) De Gennes, P. G. *C. R. Acad. Sci. Paris, Ser. B* **1975**, *281*, 101. (b) De Gennes, P. G. *Phys. Lett.* **1969**, *28A*, 725.
(4) Finkelmann, H.; Kock, H. J.; Rehage, G. *Macromol. Rapid Commun.* **1981**, *2*, 317.
(5) Küpfer, J.; Finkelmann, H. *Makromol. Chem., Rapid Commun.* **1991**, *12*, 717.
(6) Shibaev, V. P.; Finkelmann, H.; Kharitonov, A. V.; Portugal, M.; Plate, N. A.; Ringsdorf, H. *Vysokomol. Soed. A* **1981**, *23*, 919. (b) Shibaev, V. P.; Kostromin, S. G.; Plate, N. A. *Eur. Polym. J.* **1982**, *18*, 651.
(7) Finkelmann, H. *Adv. Polym. Sci.* **1984**, *60/61*, 99.
(8) Zentel, R. *Angew. Chem. Adv. Mater.* **1989**, *101*, 1437. (b) Zentel, R.; Reckert, G. *Macromol. Chem.* **1986**, *187*, 1915.
(9) Legge, C. H.; Davis, F. J.; Mitchell, G. R. *J. Phys. II* **1991**, *1*, 1253.
(10) Barclay, G. G.; Ober, C. K. *Prog. Polym. Sci.* **1993**, *18*, 899.
(11) Zubarev, E. R.; Talroze, R. V.; Yuranova, T. I.; Vasilets, V. N.; Plate, N. A. *Macromol. Chem. Rapid Commun.* **1996**, *17*, 43.
(12) Carfagna, C.; Amendola, E.; Giamberini, M. *Prog. Polym. Sci.* **1997**, *22*, 1607.
(13) Gleim, W.; Finkelmann, H. *Macromol. Chem.* **1987**, *188*, 1489.
(14) Gleim, W.; Finkelmann, H. In *Side Chain Liquid Crystalline Polymers*; McArdle, Ed.; Blacktie and Son Ltd.: Glasgow, 1989; p 287.
(15) Zentel, R. *Adv. Mater.* **1989**, 321.
(16) Davis, F. J. *J. Mater. Chem.* **1993**, *3*, 551.
(17) Brand, H. R.; Finkelmann, H. In *Physical Properties of Liquid Crystalline Elastomers*; Demus, D., Ed.; Wiley VCH: New York, 1998; pp 277−302.
(18) Terentjev, E. M. *J. Phys.: Condens. Matter* **1999**, *11*, R239.
(19) Thomsen III, D. L.; Keller, P.; Naciri, J.; Pink, R.; Jeon, H.; Shenoy, D.; Ratna, B. R. *Macromolecules* **2001**, *34*, 5868.
(20) Kundler, I.; Finkelmann, H. *Macromol. Chem. Phys.* **1998**, *199*, 677.
(21) Lacey, D.; Beattie, H. N.; Mitchell, G. R.; Pople, J. A. *J. Mater. Chem.* **1998**, *8*, 53.
(22) Whitcombe, M. J.; Gilbert, A.; Mitchell, G. R. *J. Polym. Sci., Part A: Polym. Chem.* **1992**, *30*, 1681.
(23) Creed, D.; Griffin, A. C.; Gross, J. R. D.; Hoyle, C. E.; Venkatarim, K. *Mol. Cryst. Liq. Cryst.* **1988**, *30*, 1681.
(24) Brehmer, M.; Zentel, R.; Wagenblast, G.; Siemensmeyer, K. *Macromol. Chem. Phys.* **1994**, *195*, 1891.
(25) Warner, M.; Gelling, K. P.; Vilgis, T. A. *J. Chem. Phys.* **1988**, *88*, 4008.
(26) Warner, M. In *Side Chain Liquid Crystalline Polymers*; McArdle, Ed.; Blacktie and Son Ltd.: Glasgow, 1989.
(27) Kirste, R. G.; Ohm, H. G. *Makromol. Chem., Rapid Commun.* **1985**, *6*, 179.
(28) Keller, P.; Carvalho, B.; Cotton, J. P.; Lambert, J. P.; Moussa, F.; Pepy, G. *J. Phys., Lett.* **1985**, *46*, L1065.
(29) Finkelmann, H.; Kaufhold, W.; Noirez, L.; ten Bosch, A.; Sixou, P. *J. Phys. II* **1994**, *4*, 1363.

(30) Taylor, J. E.; Romo-Uribe, A.; Libera, M. R. *Macromolecules* **2002**, *35*, 1751.
(31) Jákli, A.; Krüerke, D.; Nair, G. G. *Phys. Rev. E* **2003**, *67*, 051702.
(32) Leroux, N.; Keller, P.; Achard, M. F.; Noirez, L.; Hardouin, F. *J. Phys. II* **1993**, *3*, 1289.
(33) Hardouin, F.; Leroux, N.; Mery, S.; Noirez, L. *J. Phys. II* **1992**, *2*, 271.
(34) Schätzle, J.; Kaufhold, W.; Finkelmann, H. *Makromol. Chem.* **1989**, *190*, 3284.
(35) Küpfer, J.; Nishikawa, E.; Finkelmann, H. *Polym. Adv. Technol.* **1993**, *5*, 110.
(36) Selinger, J. V.; Jeon, H. G.; Ratna, B. R. *Phys. Rev. Lett.* **2002**, *89*, 225701.
(37) Warner, M.; Terentjev, E. M. *Prog. Polym. Sci.* **1996**, *21*, 853.
(38) Finkelmann, H.; Greve, A.; Warner, M. *Eur. J. Phys. E* **2001**, *5*, 281.
(39) Finkelmann, H.; Nishikawa, E.; Pereira, G. G.; Warner, M. *Phys. Rev. Lett.* **2001**, *87*, 015501-1.
(40) Warner, M.; Terentjev, E. M. In *LiquidCrystal Elastomers*; Clarendon Press: Oxford, in press.
(41) Josephson, R. K. *J. Exp. Biol.* **1985**, *114*, 493.
(42) Meijer, K.; Rosenthal, M. S.; Full, R. J. *Proc. SPIE, Smart Struct. Mater.* **2001**, *4329*, 7.
(43) Our earlier dielectric relaxation studies have shown that the reorientation of the liquid crystal mesogen is not the limiting factor for faster strain response. See ref 28.
(44) Shenoy, D. K.; Thomsen, D. L., III.; Srinivasan, A.; Keller, P.; Ratna, B. R. *Sens. Actuators, A* **2002**, *96*, 184.

MA034921G